Cooperative behavior of a chain of synaptically coupled chaotic neurons

M. Bazhenov [a,*], R. Huerta [b], M.I. Rabinovich [b], T. Sejnowski [a,c]

[a] Howard Hughes Medical Institute, The Salk Institute, Computational Neurobiology Laboratory, La Jolla, CA 92037, USA
[b] Institute for Nonlinear Science, University of California, San Diego, La Jolla, CA 92093-0402, USA
[c] Department of Biology, University of California, San Diego, La Jolla, CA 92093, USA

Abstract

A coupled linear chain of Hindmarsh–Rose model neurons with reciprocal inhibition between neighboring neurons exhibited synchronous oscillations in which neighboring neurons burst out-of-phase and next nearest neighbor neurons burst in-phase. The bifurcations observed inside this "out-of-phase" regime were qualitatively the same for all chains with an even number of neurons and were similar to those observed in a single isolated cell, although the organization of the behavior of a chain of coupled neurons was more regular than that of an isolated cell. When noise was added to the synaptic coupling strengths, there was less hysteresis in the system and many of the bifurcations with smaller basins of attraction were eliminated, making the system even more regular. These results suggest that in populations of bursting neurons with reciprocal inhibition, the chaotic behavior found in single cells is suppressed. Copyright © 1998 Elsevier Science B.V.

Keywords: Reciprocal inhibition; Synchronization; Chaotic oscillations

1. Introduction

The cooperative dynamics of lattices or chains of coupled generators has been the focus of considerable interest for modeling extended chemical, biological, and fluid systems. Theoretical studies of cooperative behavior include lattices of coupled oscillators [14,28], the complex Ginsburg–Landau system [17,24], lattices of coupled maps [4,22], and lattices of chaotic generators [3].

Neurons have a wide variety of voltage-dependent ionic currents that give rise to complex dynamical behaviors. In studying the dynamical properties of neural systems with model neurons coupled in lattices and

chains [2,7,10,13,23], a wide range of models for single neurons has been explored, including phase oscillators, leaky integrate-and-fire models, two-time-scale oscillators, and chaotic systems. In models of synaptically coupled neurons, the type of coupling is also important in determining the dynamical properties of the neural system.

For the diffusive-type coupling, generally used to model physical and chemical extended system, the coupling is proportional to linear differences between variables describing the states of neighboring generators. This is not a suitable model for synaptic transmission in neuronal systems, where there are complex nonlinear mechanisms with history-dependence [11]. In the simplest case where time delays and internal variables are ignored, the synaptic coupling is often

---

* Corresponding author. E-mail: bazhenov@salk.edu.

modeled as a static sigmoidal nonlinear input–output function with a threshold and saturation. The detailed features of this function depend on the type of synapse. The analysis of lattices of synaptically coupled neurons may help in understanding the spatio-temporal patterns of the neural activity found in the brain. These systems are also of interest mathematically since they exhibit new dynamical properties.

In this paper, we study the synchronization and bifurcations observed in chains of synaptically coupled chaotic bursting neurons modeled by the Hindmarsh–Rose (HR) equations [20]. In Section 2 we consider briefly a single HR cell. The dynamics of coupled HR models of bursting neurons is examined in Sections 3–6. Particular attention is given to the effect of the coupling on the chaotic behavior of the system, already present in isolated bursting neurons, when there is inhibitory coupling between the nearest neighbors along a chain. Mutually inhibitory coupling between neurons is common in central pattern generators [5,27] and is also found between inhibitory neurons in the reticular nucleus of the thalamus [29]. Both in-phase and out-of-phase synchronization of spiking has been observed in these networks, depending on the connectivity and dynamics of the coupling between the neurons as well as the properties of the neurons themselves.

A detailed analysis of out-of-phase synchronization for 2-coupled chaotic HR neurons has already been presented in [1,32]. These results are extended here with a focus on the stability and the bifurcations of the limit cycles in the out-of-phase regime.

2. The dynamic of the single Hindmarsh–Rose model neuron

The HR model [20] was developed as a qualitative model for the rhythmic bursts of spikes that occur in thalamic cells following hyperpolarizing current injection and activation of a low-threshold calcium current [29]. It is a simplification of a more detailed biophysical model that takes into account the properties of the ionic currents underlying the fast sodium spikes and the bursts of spikes that ride on a slower calcium ac-

tion potential [9]. The HR model consists of a third-order system of ordinary differential equations that is more amenable to analysis:

$$\dot{x} = F_1(x(t)) + y - z + I,$$
$$\dot{y} = F_2(x(t)) - y,$$
$$\frac{1}{r}\dot{z} = -z + S(x - C), \quad r \ll 1,$$

(1)

where the functions $F_1(x)$ and $F_2(x)$ were chosen to display the generation of bursts of spikes and are usually written in the form

$$F_1(x) = 3x^2 - x^3, \quad F_2(x) = 1 - 5x^2. \quad (2)$$

The variable $x(t)$ in (1) describes the membrane potential of the cell. The other two variables, $y(t)$ and $z(t)$, are responsible for the fast and slow ionic currents of the cell. The parameters of the model in Eq. (1) are the injected current (I), the voltage threshold (C), the influence of membrane potential on the slow dynamics (S), and the time scale for slow subsystem (r).

The set of equations (1) exhibits several forms of dynamics that depend on the values of parameters I, S and C. We choose as the basic bifurcation parameter the external current I because this variable can be measured and controlled during experiments on bursting neurons. The values of the other parameters were taken to be $S = 4$, and $C = -1.6$. Finally, the small parameter r was set to be equal to 0.0021.

Fig. 1 shows the coordinate y versus parameter I on the secant $x = 0$. To each interval $I \in (I_i^{(1)}, I_i^{(2)})$ there corresponds a stable limit cycle L_i, where $i = 1, 2, \ldots$ is the number of spikes in the burst. The cycle L_i loses its stability at the end of this interval and the cycle L_{i+1} or L_{i-1} appears. Note that, in a general case, $I_i^{(2)} > I_{i+1}^{(1)}$; therefore, there exist narrow regions of the values of the parameters $I \in (I_{i+1}^{(1)}, I_i^{(2)})$ in which two stable cycles having different numbers of spikes coexist. The result of investigation of the bifurcations of the limit cycles L_i, $i = 1, 2, \ldots$ is the following: $L_1(-1, +1)$, $L_2(-1, +1)$, $L_3(-1, +1)$, $L_4(-1, +1)$, $L_5(-1, +1)$, $L_6(-1, +1)$, $L_7(-1, +1)$, $L_8(-1, -1)$, $L_9(+1, -1)$, $L_{10}(+1, -1)$, $L_{11}(+1, -1)$, $L_{12}(+1, -1)$. The designation $L_i(-1, +1)$ means that the cycle L_i (which is stable in the interval $I \in (I_i^{(1)}, I_i^{(2)})$) has multiplier
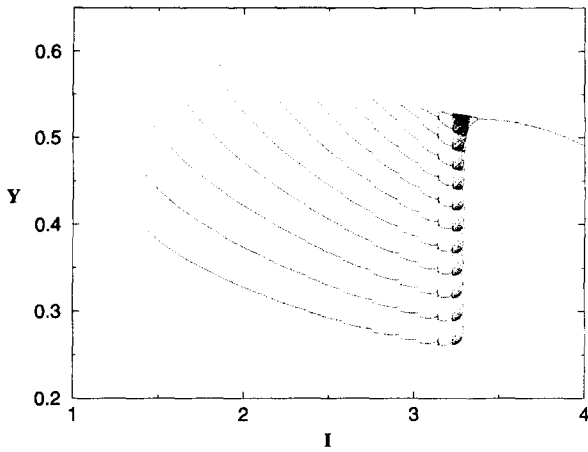
Fig. 1. One-parameter Poincare map as a function of external current I for HR model (1) of a single bursting neuron.

-1 with the second Lyapunov exponent $l > 0$ at the point $I = I_i^{(1)}$, and multiplier $+1$ at the point $I = I_i^{(2)}$.

For $I \geq 3.221$, a strange attractor emerges in the phase space of the system (1) as a result of a sequence of period-doubling bifurcations. Finally, for $I \geq 3.295$, the system in Eq. (1) ceases to generate bursts, and the dependence $x(t)$ is a chaotic sequence of spikes (see details in [15,16,21,31]).

We have considered the behavior of the system at fixed values of the parameters S and C. However, the analysis of the bifurcations presented above is qualitatively valid over a wide range of intervals of the parameters $S(I)$ and $C(I)$.

3. Poincare sections "inside synchronization" for coupled neurons

The main goal here is to characterize the different regimes of synchronization observed in the model system as a function of the strength of the inhibitory coupling and the number of coupled neurons. We focus on even numbers of coupled neurons because networks with 2-, 4- and 6-coupled HR neurons show similar transitions between limit cycles as a function of the control parameter. Models with small odd numbers of coupled HR neurons are not as similar.

The system under study is

$$\frac{dx_i}{dt} = y_i + 3x_i^2 - x_i^3 - z_i + I$$

$$- \epsilon \left(\frac{x_i + V_c}{1 + \exp((x_{i-1} - X)/\sigma)} \right.$$

$$\left. - \frac{x_i + V_c}{1 + \exp((x_{i+1} - X)/\sigma)} \right), \qquad (3)$$

$$\frac{dy_i}{dt} = 1 - 5x_i^2 - y_i,$$

$$\frac{dz_i}{dt} = -rz_i + rS(x_i + 1.6),$$

where $r = 0.0021$, $I = 3.281$ and $S = 4$. The boundary conditions are periodic, with the last element coupled to the first one.

The Poincare sections were calculated for $x_0 = 0.5$, a membrane potential that occurs during a spike. Figs. 2(a), (c), and (e) show the projection of the Poincare section on the coordinate z for even number of coupled HR models for increasing (upper figure) and decreasing (lower figure) values of the control parameter.

For small values of the coupling parameter $\epsilon < \epsilon_{cr} = \epsilon_9^{(1)}$ the system behavior is generally chaotic. More detailed analysis reveals that there exist narrow intervals in the strength of the coupling ϵ where the behavior of the system is regular. Within these intervals the model neurons display "in-phase" synchronized oscillations. The behavior of the system changes completely for $\epsilon > \epsilon_{cr}$. Beginning at $\epsilon = \epsilon_{cr}$, the system demonstrates regular oscillations with "out-of-phase" synchronization between the elements. Increasing the strength of the coupling for $\epsilon > \epsilon_{cr}$ produces a sequence of local bifurcations of the periodic orbits. At every bifurcation point, $\epsilon = \epsilon_k^{(1)}$, the periodic orbit L_k with k spikes on the burst loses stability and the system evolves to a periodic orbit L_{k+1} with $k + 1$ spikes. If ϵ is decreased then the opposite behavior is observed (at the point $\epsilon = \epsilon_{k+1}^{(2)}$ the periodic regime L_{k+1} loses stability). Since $\epsilon_{k+1}^{(2)} < \epsilon_k^{(1)}$ for all k, in the neighborhood of the bifurcation point the stable periodic orbits with different number of spikes (and consequently with different periods) coexist, and the initial conditions determine which regime is realized, a form of hysteresis.
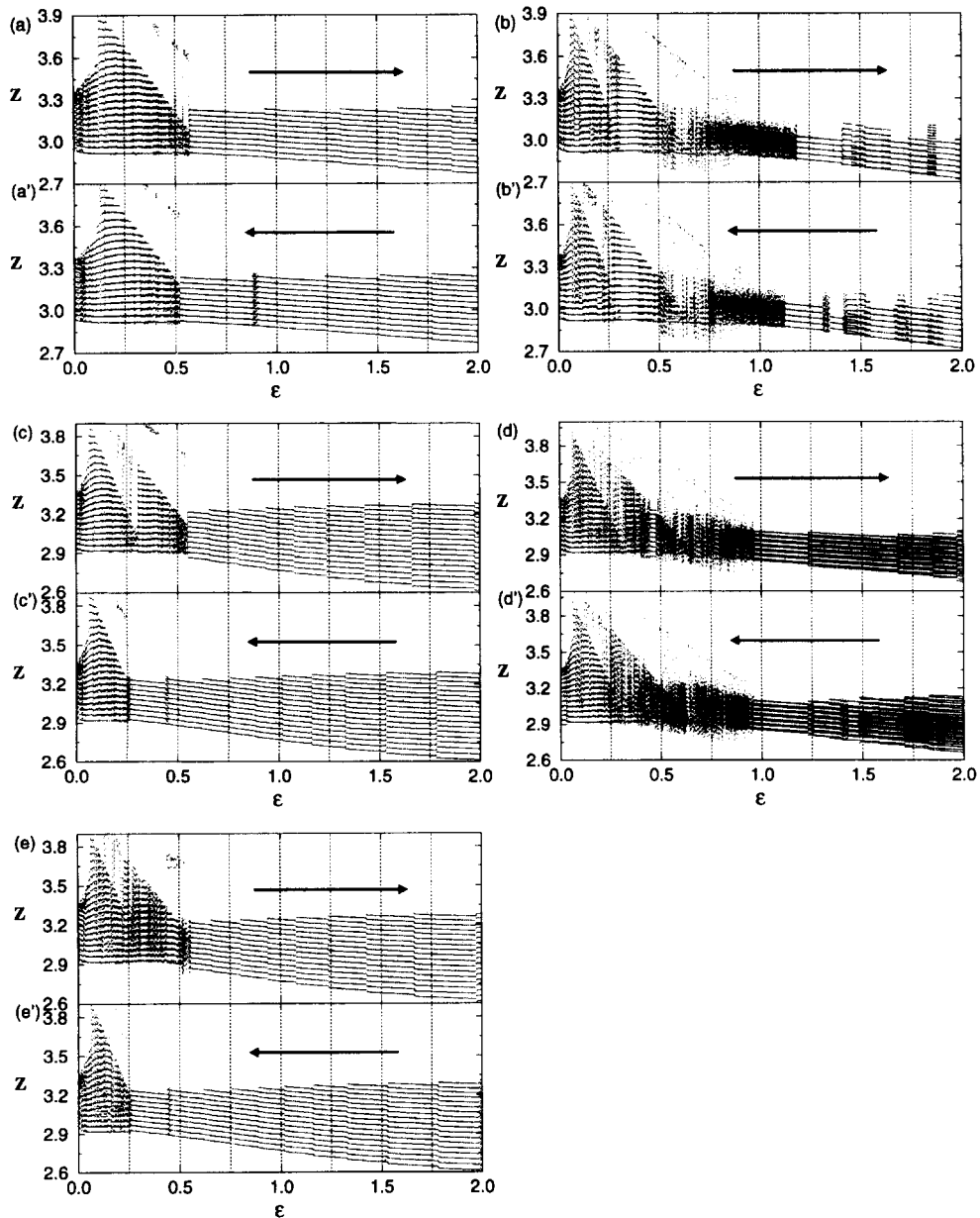
Fig. 2. One-parameter Poincare maps as a function of the strength of the reciprocal inhibitory coupling ϵ between neighboring neurons in a linear chain for: (a) two; (b) three, (c) four, (d) five, and (e) six HR model cells. The arrow indicates the direction in which the control parameter ϵ was varied to produce the map.

For 4- and 6-coupled inhibitory neurons, the same qualitative behavior is observed as for the two-neuron case. The main difference is that the number of inhibitory inputs for neurons in the middle of the chain has doubled, providing stronger input; this results in a larger number of spikes in each burst for the same value of the coupling strength compared to the two-neuron case.

It is important to note that for $\epsilon > \epsilon_{cr}$, the bifurcations occur during out-of-phase synchronization and only modify this behavior by changing the number of spikes in a burst. Hence, we call this regime "bifurcation inside synchronization".

These results show the similarity of the behavior not only between systems with 2, 4 and 6 coupled neurons but also between these systems and a single HR cell. In all cases, increasing one of the parameters (external current for a single cell and strength of the coupling for coupled cells) results in a similar sequence of bifurcations between cycles with different numbers of spikes per burst (compare Figs. (1) and (2)).

For 3 coupled inhibitory neurons, the behavior is not as regular as the case for two neurons (see Fig. 2(b)). First, much stronger coupling is needed to make the behavior regular. Second, the sequence of limit cycles is not ordered as before. Finally, the sequence of attractors observed for increasing values of the control parameter is not the same as for decreasing values. As a consequence, multistability occurs over broad intervals of the inhibitory coupling strength. The complexity of the system with 3 coupled HR neurons is thus significantly greater than that for 2 coupled neurons. The number of spikes is different on successive bursts, which implies a lower degree of symmetry than found with an even number of neurons in the chain.

In Fig. 2(d) the Poincare section for 5-coupled neurons, a strong coupling is needed to achieve a regular behavior, but less strength is required than for 3-HR-coupled neurons. Although multistability is still evident, the appearance of the Poincare section is more similar to the cases with even numbers of neurons. As the number of neurons in the chain becomes large, the behavior of even and odd chains should converge.

The multistability observed in system with an odd number of coupled neurons can be explained by taking into account the translation symmetry of the system and the periodic boundary conditions. For an even number of neurons in the out-of-phase regime, the translation operator to the chain produces the same limit cycles, where the translation operator is defined as σ : $(x_{i+1}, y_{i+1}, z_{i+1}) \rightarrow (x_i, y_i, z_i)$ for $i = 1, \ldots, N$ with $i = N + 1 \rightarrow 1$. There must be a single limit cycle for any initial condition. In contrast,

for odd numbers of elements in the chain in the out-of-phase regime, application of the translation operator produces a different limit cycle (because the number of spikes per burst is not the same for all units). In the case for an odd number of neurons, N limit cycles can be realized for different initial conditions.

4. Local bifurcations for model of coupled neurons

Consider in detail the local bifurcations of the limit cycles in the system of 2-, 4- and 6-coupled elements. We are mainly interested in analyzing the case $\epsilon > \epsilon_{cr}$ when the stable regimes of the out-of-phase oscillations are observed in the system and increasing the control parameter ϵ transforms the regime of the oscillations with N spikes to the regime with $N + 1$ spikes. For 2-coupled cells only the oscillations with $N > 8$ are stable and the bifurcations satisfy: $L_{9,10}(-1, +1)$, $L_k(+1, +1)$, $k > 10$. Thus, all bifurcations points $\epsilon_k^{(1,2)}$ are a saddle-node type except for two points $\epsilon_9^{(1)}$ and $\epsilon_{10}^{(1)}$ which correspond to flip bifurcations of the cycles L_9 and L_{10}.[1] These points have an interesting feature. In both cases when ϵ decreases the highest multiplier achieves a value of $+1$ (saddle-node bifurcation) before flipping to a value of -1 (Fig. 3(a)). At the critical point ϵ_k^0 ($\mu(\epsilon_k^0) = +1$) the cycle L_9 (L_{10}) has neutral stability in one of the directions. However, the bifurcation does not occur at this point and a further decrease of the control parameter induces a smooth decrease of the multiplier. In the vicinity of the points $\epsilon_k^{(1)}$, $k = 9, 10$, the system undergoes a series of period-doubling bifurcations that lead to the formation of a strange attractor [25,26].

The local bifurcations observed in chains with four and six neurons are exactly the same as the ones found in the two-neuron model: $L_{9,10}(-1, +1)$, $L_k(+1, +1)$, $k > 10$. In particular, the dynamics of the model in the vicinity of the flip bifurcation points $\epsilon_9^{(1)}$ and $\epsilon_{10}^{(1)}$ has a profile highly similar to that for 2-coupled neurons (Figs. 3(b) and (c)). This is not surprising since the Poincare sections for the regions

---

[1] The cycle L_k is stable in the region $\epsilon \in (\epsilon_k^{(1)}, \epsilon_k^{(2)})$.
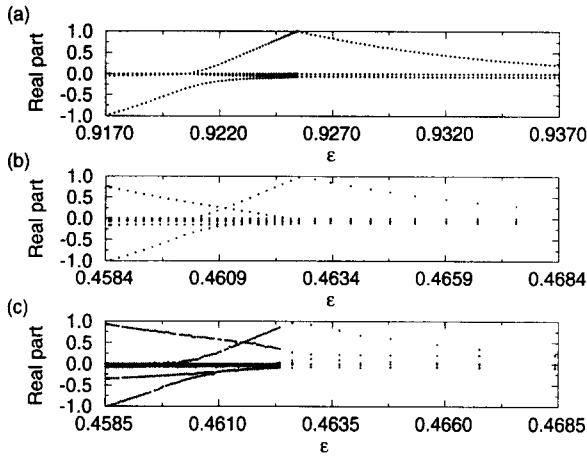
(a)

(b)

(c)

Fig. 3. Real part of the multipliers for: (a) 2-; (b) 4-; and (c) 6-coupled HR models as a function of increasing inhibitory coupling ϵ for a period-doubling bifurcation. Note the similarity of the system dynamics in the vicinity of the bifurcation points.

of the chaotic dynamics near the points $\epsilon_9^{(1)}$ and $\epsilon_{10}^{(1)}$ are so similar (see Fig. 2).

Does the similarity between the models with two and four neurons generalize to even larger networks? We simulated a chain of 50 reciprocally inhibitory coupled elements (not shown) and found the same "out-of-phase" patterns. This suggests that some of the conclusions reached for chains with an even number of neurons may hold for larger chains, and perhaps even in the limit as the number of neurons goes to infinity. However, there may be important differences in these models that need to be further investigated.

5. Two-parametric bifurcation diagram for 2-coupled neurons

The external current I was used as a control parameter for one-parameter bifurcation diagrams in Section 2. To analyze the relative role of this parameter in comparison to the strength of the coupling, we examined a two-parameter bifurcation diagram, $I(\epsilon)$, for 2-coupled neurons (see Fig. 4). The bifurcation points $\epsilon_k^{(1,2)}$ have a codimension-1 and transformed to the curves $\epsilon_k^{(1,2)}(I)$ on the plane $I(\epsilon)$. The analysis of the plane $I(\epsilon)$ reveals some interesting features of system (3). First, the bifurcation points $\epsilon_k^{(1)}$ and $\epsilon_k^{(2)}$
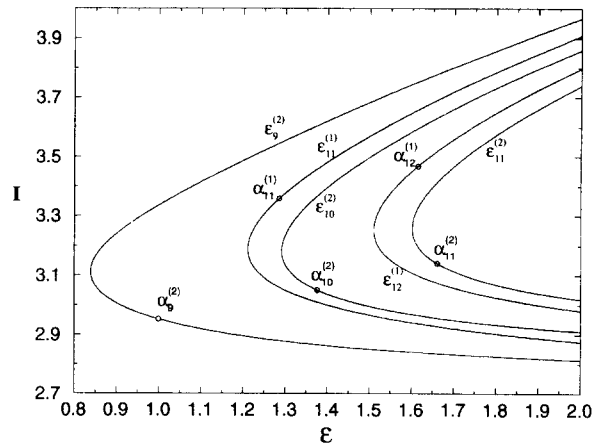

Fig. 4. Two-parameter bifurcation diagram as a function of the external current I and the inhibitory coupling strength ϵ for 2-coupled HR models. The points $a_k^{(1,2)}$ correspond to bifurcations of codimension-2. The upper segments of the curves ϵ_9^2, ϵ_{10}^2 and ϵ_{11}^2 (above of the points α_9^2, α_{10}^2 and α_{11}^2, respectively) correspond to a saddle-node bifurcation and the lower segments of the same curves correspond to the Neimark–Sacker bifurcation. In contrast, the upper segments of the curves ϵ_{11}^1 and ϵ_{12}^1 (above of the points α_{11}^1 and α_{12}^1, respectively) correspond to the Neimark–Sacker bifurcation and the lower segments of the same curves correspond to a saddle-node bifurcation.

corresponding to the increasing $(\epsilon_k^{(1)})$ and decreasing $(\epsilon_k^{(2)})$ values of the control parameter have the same type (saddle-node) only in the narrow interval of the values of the parameter $I \approx (3.2, 3.4)$. This interval includes all regions of the chaotic dynamics observed in single HR model (see Fig. 1).

The analysis of the two-parameter bifurcation diagram shows another interesting property of system (3).Outside the previously mentioned interval $I \approx (3.2, 3.5)$ the bifurcation curves are almost parallel to each other and there is an almost linear relationship $\epsilon_k^{(1,2)} \cong \epsilon_{k0}^{(1,2)} + \alpha^{(1,2)}I$. In this region any change of the parameter ϵ can be balanced (from the point of view of the stability of the limit cycles) by a proportional change of the parameter I. This last point is not trivial if we consider that I is the amplitude of the effective external current permanently applied to the neurons in the chain and ϵ defines the amplitude of the synaptic current, which is nonzero during the firing of the neighboring cells. Thus, from the point of view of the local stability of periodic orbits (at least),

a change in the amplitude of synaptic current pulses is equivalent to adding some constant current, such as a leak current. In other words, the effects of changes of the synaptic conductances between neurons (a local property) can be compensated by external currents, which could be achieved by a global neuromodulator.

6. Effects of noise on bifurcations in the model of coupled neurons

The model of coupled neurons (3)considered so far does not take into account the noise that is present in biological systems as a consequence of fluctuations in the ionic currents in the neurons and the synapses. The influence of noise on the dynamics of the system is particularly strong near critical points (bifurcations), where the system is sensitive to small changes in the input and the noise can switch the behavior from one regime to another. To test the effect of the noise we investigated the dynamics of a modified system

$$\frac{dx_i}{dt} = y_i + 3x_i^2 - x_i^3 - z_i + I - (\epsilon + \eta(t))$$

$$\times \left(\frac{x_i + V_c}{1 + \exp(x_{i-1} - X/\sigma)} \right.$$

$$\left. - \frac{x_i + V_c}{1 + \exp(x_{i+1} - X/\sigma)} \right), \tag{4}$$

$$\frac{dy_i}{dt} = 1 - 5x_i^2 - y_i,$$

$$\frac{dz_i}{dt} = -rz_i + rS(x_i + 1.6),$$

where $\eta(t)$ is a zero-mean additive white noise with variance σ. This model was examined near the bifurcation point corresponding to the transition between the regimes L_9 and L_{10}. Qualitatively different behavior was observed in the transition between regimes in the presence of noise compared with the absence of noise. Without noise, the system displayed strong hysteresis, as shown in Fig. 5(a) and (b). In presence of noise, shown in Fig. 5(c) and (d) the hysteresis region was smaller and the behavior of the system showed less dependence on the initial conditions. In the presence of noise, the fluctuations in the membrane po-

tential was larger near bifurcation points compared to when the system was far from a bifurcation. Near bifurcation points, the system could suddenly "switch" between different regimes (Fig. 5(d)). Thus, noise prevented the appearance of attractors with small basins and, therefore, reduced the multistability of the system.

7. Discussion

Complex rhythmic behaviors have been observed in a wide range of biological systems including central pattern generators [19,27], thalamocortical systems [9,12,18,29] and the cerebellum [30]. The focus of this paper has been on the qualitative properties of bursting neurons and the influence of mutual inhibitory coupling on cooperative states.

Reciprocal inhibition leads to out-of-phase oscillation of neighbor neurons in a linear chain of model neurons based on bursting neurons in the thalamus. The number of spikes in a burst increases as the strength of the reciprocal inhibition is increased. The model with coupled neurons displayed less chaotic behavior than that observed in an isolated model neuron. We showed that the codimension-1 bifurcations lead to the regularization and switching between periodic regimes with different numbers of spikes. The same phenomenon may occur in other more complex systems that display synchronous activity, such as spindling in thalamocortical systems [3].

Chains of bursting neurons coupled synaptically exhibit a new type of organized phenomenon not found in models with traditional diffusive coupling. Inhibitory coupling between bursting neurons produces several types of out-of-phase oscillations. The nonlinear synaptic coupling allows limit cycles to occur in the coupled model even though single neurons are situated in their chaotic regime. The coupled model, which nonetheless exhibits the same types of bifurcation that appear in the isolated cell, also has smaller regions of bistability near the saddle-node bifurcations for an even number of coupled neurons. This does not occur in chains with an odd number of neurons.
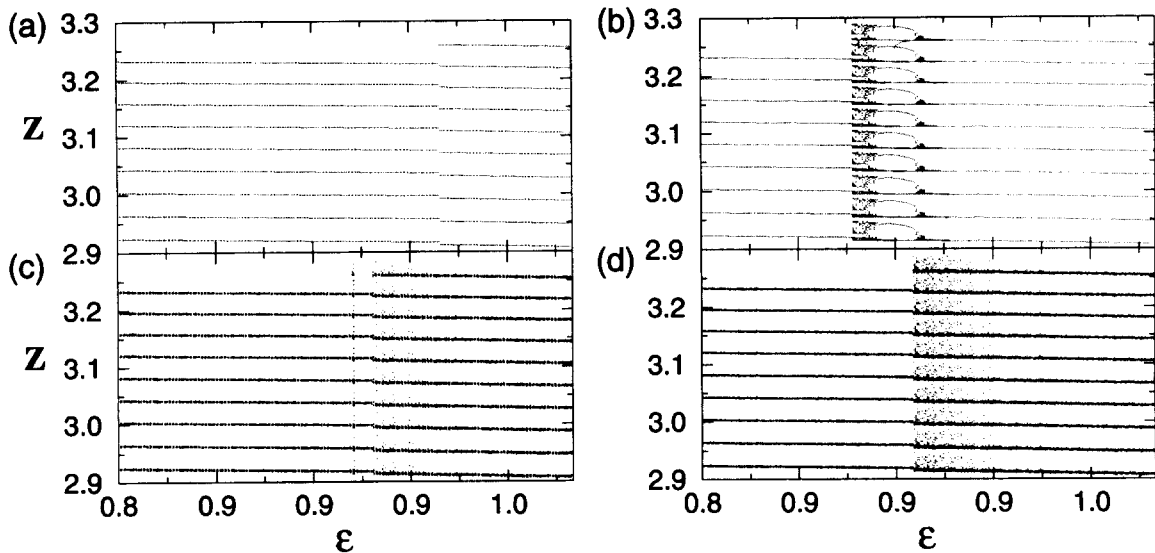
Fig. 5. One-parameter Poincare map as a function of the strength of the inhibitory coupling , ϵ, for 2-coupled HR models: (a) without noise for increasing values of the coupling; (b) without noise for decreasing values of the strength of the coupling; (c) including additive white noise with variance 0.08 in the synaptic strength for increasing values of the inhibition; and (d) with additive white noise with variance 0.08 in the synaptic strength, ϵ, for decreasing values of the inhibition.

We calculated the bifurcations for a chain of 2, 4 and 6 neurons. They were the same as those in an isolated bursting neuron, including the same dependence of the multipliers and the period as a function of the control parameter. However, the stability of longer chains of coupled neurons needs further investigation. It is possible that instabilities will appear, such as the modulation instabilities that are typical for extended systems [17]. For example, it has been shown that the homogeneous solution of two-dimensional network of synaptically coupled inhibitory and excitatory neurons becomes unstable and spatio-temporal chaos appears if the size of the network exceeds some critical value [2].

The results reported here are a starting point for a more detailed analysis of the bifurcations in bursting systems of coupled inhibitory.

Acknowledgements

References

[1] H.D.I. Abarbanel, R. Huerta, M.I. Rabinovich, P. Rowat, N. Rulkov, A.I. Selverston, Neural Comput. 8 (1996) 1567.

[2] H.D.I. Abarbanel, M.I. Rabinovich, A. Selverston, M.V. Bazhenov, R. Huerta, L. Rubchinsky, M. Sushick, Uspekhi Fizicheskii Nauk 166 (4) (1996) 363; Transl. in: Physics-Uspekhi 39 (4) (1996) 337.

[3] L. Brunnet, H. Chate, P. Manneville, Physica D 78 (1994) 141.

[4] L.A. Bunimovich, Ya.G. Sinai, Nonlinearity 1 (1988) 494.

[5] R.L. Calabrese, F. Nadim, O.H. Olsen, J. Neurobiol. 27 (1995) 390–402.

[6] D. Contreras, A. Destexhe, T.J. Sejnowski, M. Steriade, Corticothalamic feedback controls the spatiotemporal coherence of a thalamic oscillation, Science 274 (1996) 771.

[7] A. Corral, C.J. Perez-Vicente, A. Diaz-Guilera, A. Arenas, Phys. Rev. Lett. 75 (1995) 3697.

[8] A. Destexhe, Phys. Rev. E 50 (2) (1994) 1594.

[9] A. Destexhe, T. Bal, D.A. McCormick, T.J. Sejnowski, J. Neurophysiol. 76 (3) (1996) 2049.

[10] A. Destexhe, D. Contreras, T.J. Sejnowski, M. Steriade, J. Neurophysiol. 83 (1994) 803.

[11] A. Destexhe, Z.F. Mainen, T.J. Sejnowski, J. Comput. Neurosci. 1 (1994) 195.

[12] A. Destexhe, T.J. Sejnowski, Synchronized oscillations in thalamic networks: Insights from modeling studies, in: M. Steriade, E.G. Jones, D.A. McCormick (Eds.), Thalamus, Elsevier, Amsterdam, 1998.

[13] A. Diaz-Guilera, A. Arenas, C.J. Perez-Vicente, A. Corral, Physica D 103 (1997) 419.

[14] B. Ermentrout, Physica D 82 (1995) 154.

[15] Y.S. Fan, T.R. Chay, Phys. Rev. E 51 (1995) 1012.

[16] Y.S. Fan, A.V. Holden, Chaos, Solitons and Fractals 3 132.

[17] A.V. Gaponov-Grekhov, M.I. Rabinovich, Nonlinearity in Action, Springer, Berlin, 1992.

[18] D. Golomb, X.J. Wang, J. Rinzel. J. Neurophysiol. 75 (1996) 750.

[19] R.M. Harris-Warrick, L.M. Coniglio, N. Barazangi, J. Guckenheimer, S. Gueron, J. Neurosci. 15 (1) (1995) 342.

[20] J.L. Hindmarsh, M. Rose, Proc. Roy. Soc. London B 221 (1984) 87.

[21] A.V. Holden, Y.S. Fan, Chaos, Solitons and Fractals 2 221.

[22] K. Kaneko, Physica D 34 (1989) 1.

[23] K. Kaneko, Theory and Applications of Coupled Map Lattices, Wiley, New York, 1993.

[24] Y. Kuramoto, Chemical Oscillations, Waves and Turbulence, Springer, Berlin, 1984.

[25] Y. Kuznetsov, Elements of Applied Bifurcation Theory, Springer, Berlin, 1995.

[26] Y. Pomeau, P. Manneville, Commun. Math. Phys. 74 (2) (1980) 189.

[27] A.I. Selverston (Ed.), Model Neural Networks and Behavior, Plenum Press, New York, 1985.

[28] D. Somers, N. Kopell, Physica D 89 (1995) 169.

[29] M. Steriade, E.G. Jones, R.R. Llinas (Eds.), Thalamic Oscillations and Signaling, Wiley, New York, 1990.

[30] I. Sugihara, E.J. Lang, R. Llinas, Eur. J. Neurosci. 7 (4) (1995) 521.

[31] X.J. Wang, Physica D 62 (1993) 263.

[32] R. Huerta, M.I. Rabinovich, H.O.I. Abarbanel, M. Bazhenov, Phys. Rev. E 55 (1987) R 2108.